

# Nuclear spectroscopy at KISS

Yoshikazu HIRAYAMA<sup>†1</sup>, Yutaka WATANABE<sup>1</sup>, Momo MUKAI<sup>2,1,3</sup>, Hyunsuk CHOI<sup>4</sup>,  
Murad AHMED<sup>\*2,1</sup>, Hironobu ISHIYAMA<sup>1,2</sup>, Sunchan JEONG<sup>1,5</sup>, Sota KIMURA<sup>2,1,3</sup>,  
Junyoung MOON<sup>5</sup>, Michihiro OYAIZU<sup>1</sup>, Jinhyung PARK<sup>5</sup>, Peter SCHURY<sup>1</sup>, Michiharu  
WADA<sup>1</sup>, and Hiroari MIYATAKE<sup>1</sup>

<sup>1</sup>Wako Nuclear Science Center (WNSC), Institute of Particle and Nuclear Studies  
(IPNS), High Energy Accelerator Research Organization (KEK), Saitama 351-0198,  
Japan

<sup>2</sup>Graduate School of Pure and Applied Sciences, University of Tsukuba, Ibaraki  
305-0006, Japan

<sup>3</sup>Nishina Center for Accelerator-Based Science, RIKEN, Wako, Saitama 351-0198, Japan

<sup>4</sup>Department of Physics and Astronomy, Seoul National University, Seoul 08826,  
Republic of Korea

<sup>5</sup>Rare Isotope Science Project, Institute for Basic Science (IBS), Daejeon, 305-811,  
Republic of Korea

<sup>†</sup>Email: yoshikazu.hirayama@kek.jp

## Abstract

We developed the KEK Isotope Separation System (KISS) for the nuclear spectroscopy of the nuclei in the vicinity of  $N = 126$ . The spectroscopy is important not only to study the nuclear structure but also to understand the explosive astrophysical environment for the formation of the third peak in the observed solar  $r$ -abundance pattern. We report the experimental results of  $\beta$ - $\gamma$  spectroscopy and in-gas-cell laser ionization spectroscopy for the nuclei in this heavy region.

## 1 Introduction

The study of the  $\beta$ -decay half-lives and nuclear masses of waiting-point nuclei with  $N = 126$  is crucial to understand the explosive astrophysical environment for the formation of the third peak in the observed solar abundance pattern, which is produced by a rapid neutron capture process ( $r$ -process) [1]. For the nuclear spectroscopy in this heavy region, we have developed the KEK Isotope Separation System (KISS) [2, 3]. The KISS is an argon-gas-cell-based laser ion source combined with an on-line isotope separator [4]. The nuclei around  $N = 126$  are produced by multi-nucleon transfer reactions (MNT) [5] of  $^{136}\text{Xe}$  beam and  $^{198}\text{Pt}$  target [6]. For  $\beta$ - $\gamma$  decay spectroscopy to deduce the half-lives, we developed high-efficiency detector system, which consists of new gas counter (MSPGC) [7, 8] and Super Clover Ge detectors (SCGe). For precise mass measurement, we installed a multi-reflection time-of-flight mass spectrograph (MRTOF-MS) [9]. The KISS facility enabled us to perform in-gas-cell laser ionization spectroscopy from radiation measurements by using the  $\beta$ - $\gamma$  decay detectors and from ion counting particle-identified by using the MRTOF-MS. Here, we report the present status and experimental results at KISS.

---

\*Present address: Department of Physics, Bangladesh University of Textiles, Dhaka 1208, Bangladesh

## 2 KISS

Figure 1 shows a schematic layout of KISS installed at the RIBF facility in RIKEN. It consists of the gas-cell system shown in the red box in Fig. 1, the laser system, the mass-separator system, the detector station for decay spectroscopy, and the MRTOF-MS for mass measurements.

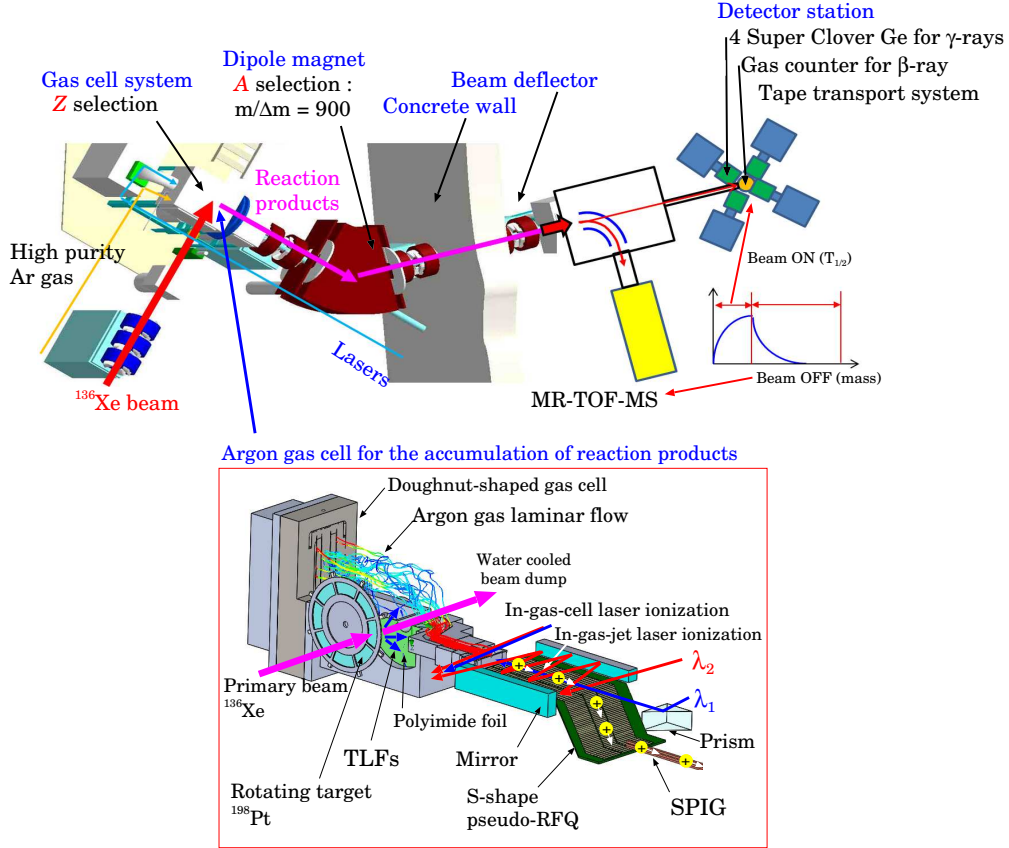


Figure 1: Schematic view of KISS (top), and the KISS gas cell shown in the red box (bottom).

### 2.1 KISS gas cell system

A primary beam of  $^{136}\text{Xe}^{20+}$  ( $\sim 7$  MeV/nucleon, 50 pA) irradiates production targets such as enriched  $^{198}\text{Pt}$  (purity 91.63% and thickness  $12.5$  mg/cm $^2$ ),  $^{\text{nat}}\text{Pt}$ , and  $^{\text{nat}}\text{W}$  [6]. Then, the primary beam passes through the beam pipe of the doughnut-shaped gas cell [3] (see Fig. 1) without entering the gas cell, where reaction products of interest are stopped. Finally, the beam is stopped at a water-cooled beam dump, which is placed far from the KISS gas cell.

For increasing the production yield, the doughnut-shaped gas cell (see Fig. 1) was developed to avoid the primary beam passing through the gas cell, otherwise plasma effects [18] significantly reduce the efficiency to extract the reaction products from the gas cell. Only the target-like fragments (TLFs) can be implanted into the gas cell with high efficiency, owing to the characteristic large emission angles of TLFs [2]. Then, the TLFs neutralized in the argon gas were transported toward the exit by an optimized argon gas laminar flow [3]. We employed two kinds of two-color two-step laser resonance ionization techniques for selecting the atomic number  $Z$ . By applying the in-gas-cell and in-gas-jet laser ionization techniques, we can produce

singly charged ions in this heavy region with  $Z = 70-78$  for  $\beta$ - $\gamma$  spectroscopy, hyperfine structure (HFS) and mass measurements even though these elements are refractory. The in-gas-cell laser ionization technique is applied for the spectroscopic work which requires higher yields. On the other hand, in-gas-jet laser ionization technique [19], which can selectively ionize ground and isomeric states of the nuclei, is used for much more precise nuclear spectroscopic works.

The laser-produced singly charged ( $q = 1$ ) ions were transported through a S-shaped pseudo-RFQ (S-RFQ) and sextupole ion guide (SPIG), and were accelerated with an energy of 20 kV. Their mass-to-charge ratio ( $A/q$ ) was selected by a dipole magnet with  $A/\Delta A = 900$ . Finally, one kind of isotope was transported to the detector station placed at the neighboring experimental hall for the nuclear spectroscopy.

## 2.2 Detector station and MRTOF-MS

The detector station has a tape transport device to avoid accumulation of the radioactivity from the daughter nuclei of the separated nuclides under the pulsed beam operation of KISS. An aluminized Mylar tape was moved at the end of each measurement cycle to remove unwanted radioactivity from the detection area. We developed high-efficiency and low-background gas counter, named multi-segmented proportional gas counter (MSPGC) [7, 8], in order to perform  $\beta$ - $\gamma$  and laser spectroscopic studies by detecting  $\beta$ -particles, X-rays, and internal conversion electrons emitted from rare reaction products. Four Super Clover Ge detectors were installed to detect  $\beta$ -delayed  $\gamma$ -rays and  $\gamma$ -rays of de-excitation transitions from isomeric states. The absolute detection efficiency for  $\gamma$ -rays with an energy of 400 keV and 1000 keV was measured as high as 14% and 10%, respectively, owing to the close setup geometry of approximately 50 mm from the implantation position on the tape.

We can transport KISS beam to the MRTOF-MS by using an electric deflector for producing pulsed beam during the decay curve measurement at the decay station. Half-lives and masses can be simultaneously measured in one experiment as shown in Fig. 1. The measured mass resolving power  $R_m$  is more than 200,000 which indicates that only 100-ion accumulation is sufficient to determine a nuclear mass with the mass precision  $\delta m/m = 10^{-6}$  ( $\delta m \approx 100$  keV). The value of  $\delta m \approx 100$  keV satisfies with an astrophysical requirement to study the explosive astrophysical environment. The MRTOF-MS has been successfully developed and applied not only to mass measurements [9] but also to the particle identifications for further nuclear spectroscopy such as hyperfine measurements.

## 3 Experimental results

Due to the difficulties in the production and ion-extraction of the refractory nuclei in this heavy region ( $Z = 70-78$  and  $N \leq 126$ ), spectroscopic study has been scarcely carried out, especially, no laser spectroscopic data for the neutron-rich nuclei (limited to stable nuclei and neutron-deficient nuclei). However, we can access the neutron-rich nuclei of these refractory elements by selecting appropriate production targets at the KISS facility. By using enriched  $^{198}\text{Pt}$ , natural platinum and tungsten targets, we extracted 17 neutron-rich nuclei from the KISS gas cell for nuclear spectroscopic works. We have successfully performed decay spectroscopy of  $^{195,196,197,198}\text{Os}$  [10, 11, 12], high-K isomer  $^{187}\text{Ta}$  [13] and  $^{192}\text{Re}$  [14], and also perform in-gas-cell laser ionization spectroscopy of  $^{199g,199m}\text{Pt}$  [15],  $^{196,197,198}\text{Ir}$  [16], and  $^{194,196}\text{Os}$  [17] for determining the magnetic moments and the change of the charge-radii (deformation parameters). We plan to perform the laser spectroscopy for these nuclei as well as the  $\beta$ - $\gamma$  spectroscopy and mass measurements intensively and systematically.

In the following sections, we introduced experimental results of the laser spectroscopy for

$^{196,197,198}\text{Ir}$  [16] and the  $^{194,196}\text{Os}$  [17]. In the case of in-gas-cell laser ionization spectroscopy, the measured laser resonance spectrum is generally broadened by a pressure broadening due to the atomic collision with argon atoms in the gas cell (the gas pressure  $\sim 75$  kPa). However, we can deduce an isotope shift value from the measured center of gravity frequency of atomic transitions and magnetic dipole moment which governs the resonance width and structure. These physics quantities are very important to discuss the nuclear deformation and structure including a wave-function.

### 3.1 Laser spectroscopy of $^{196,197,198}\text{Ir}$ isotopes

We successfully performed in-gas-cell laser ionization spectroscopy of  $^{196,197,198}\text{Ir}$  [16] for determining the magnetic moments and the change of the charge radii (deformation parameters). Figure 2 shows the measured HFS spectra by detecting the  $\beta$ -rays emitted from each isotope ( $T_{1/2} \sim 10$  min) as a function of laser wavelength.

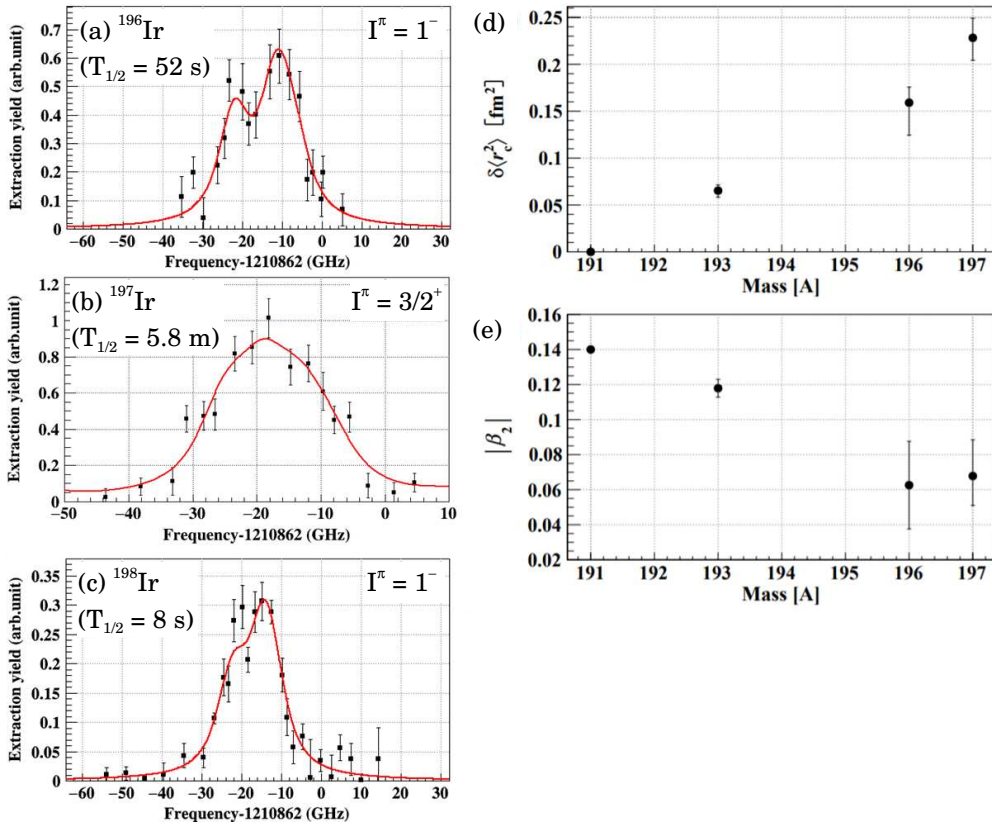


Figure 2: Measured HFS spectra of (a)  $^{196}\text{Ir}$ , (b)  $^{197}\text{Ir}$ , and (c)  $^{198}\text{Ir}$ . The red lines indicate the best fit lines with each spin-parity value. (d) Evaluated change of charge radii, and (e) deduced deformation parameters.

By fitting the measured HFS spectra, we can evaluate the change of charge radii and deformation parameters as shown in Figs. 2-(d) and (e), respectively, from the measured isotope shifts, and discuss the systematic trend [16]. The magnetic moments ( $\mu_{\text{exp}}$ ) with spin-parity  $I^\pi$  can be extracted from the measurements as shown in Table 1, and we can suggest the wave-function of each isotope from the theoretical  $\mu_{\text{calc}}$  calculated by applying strong-coupling model [20]. In order to determine the magnetic moments with spin-parity and wave-functions

more precisely and explicitly, we have been developing an in-gas-jet collinear laser ionization spectroscopy technique [19].

Table 1: Results of the in-gas-cell laser ionization spectroscopy of  $^{196,197,198}\text{Ir}$  [16].

Nuclide	$I^\pi$	$\mu_{\text{exp}} (\mu_N)$	$\mu_{\text{calc}} (\mu_N)$	suggested wave-function
$^{196}\text{Ir}$	$1^-$	$+0.31^{+0.04}_{-0.20}$	$+0.15^{+0.09}_{-0.03}$	$\pi 3/2^+[402] \otimes \nu 1/2^- [501]$
	$2^-$	$+0.34^{+0.05}_{-0.14}$	$+0.39^{+0.11}_{-0.04}$	$\pi 3/2^+[402] \otimes \nu 1/2^- [501]$
$^{197}\text{Ir}$	$3/2^+$	$+0.23^{+0.10}_{-0.03}$	$+0.23^{+0.04}_{-0.04}$	$\pi 3/2^+[402]$
$^{198}\text{Ir}$	$1^-$	$+0.13^{+0.10}_{-0.02}$	$+0.16^{+0.09}_{-0.04}$	$\pi 3/2^+[402] \otimes \nu 1/2^- [510]$

### 3.2 Laser spectroscopy of $^{194,196}\text{Os}$ isotopes with the assist of MRTOF-MS

Although we have measured the HFS spectra of short-lived ( $T_{1/2} \sim 10$  min) isotopes by detecting the  $\beta$ - and  $\gamma$ -rays at the KISS facility successfully, it was difficult to measure the HFS spectra of isotopes with  $T_{1/2} > 1$  h by detecting the decay radiations in a limited beam time. However, we can efficiently measure the laser resonance spectra of these isotopes thanks to an ion counting by using the MRTOF-MS without waiting for the radiation decays. The MRTOF-MS can identify clearly the isotopes from the mass-dependent time-of-flight (TOF) spectrum as shown in Fig. 3-(a).

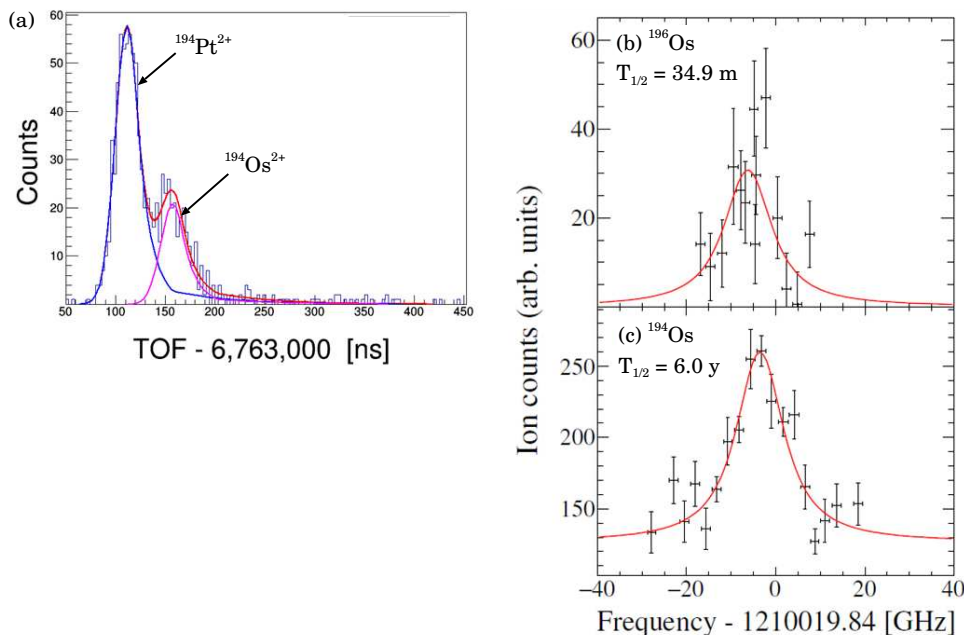


Figure 3: (a) Measured TOF spectrum of laser-induced  $^{194}\text{Os}^{2+}$  (doubly charged in the MRTOF-MS system) with survived ion of non laser-resonant  $^{194}\text{Pt}^{2+}$  emitted from the platinum production target. Measured laser resonance spectra of (b)  $^{196}\text{Os}$  and (c)  $^{194}\text{Os}$ .

To study the nuclear structures, we successfully measured the laser resonance spectra of  $^{196}\text{Os}$  ( $I^\pi = 0^+$ ,  $T_{1/2} = 34.9$  m) and  $^{194}\text{Os}$  ( $I^\pi = 0^+$ ,  $T_{1/2} = 6.0$  y), as shown in Figs. 3-(b) and (c) respectively, to determine the change in charge radii and the deformation parameters

by using the in-gas-cell laser ionization spectroscopy technique assisted by MRTOF-MS [17]. By comparing the evaluated deformation parameters with theoretical values, we found that  $^{194}\text{Os}$  nucleus is oblatelly deformed and  $^{196}\text{Os}$  nucleus would not be pure axially deformed rotor. Further systematic measurements of osmium isotopes are planed.

## 4 Summary

The KEK Isotope Separation System (KISS) was installed at RIKEN to perform nuclear spectroscopy of neutron-rich isotopes with neutron numbers around 126 for applications in astrophysics. We can successfully extract the neutron-rich isotopes produced by the MNT reactions from the KISS gas cell. We performed decay spectroscopy of  $^{195,196,197,198}\text{Os}$ ,  $^{187}\text{Ta}$ , and  $^{192}\text{Re}$  isotopes. By using in-gas-cell laser ionization spectroscopy technique, we measured the HFS spectra of  $^{199g,199m}\text{Pt}$ ,  $^{196,197,198}\text{Ir}$ , and  $^{194,196}\text{Os}$  isotopes. As the further spectroscopic studies at KISS, we plan to perform mass measurements by using MRTOF-MS and precise in-gas-jet laser ionization spectroscopy additionally.

## Acknowledgments

This experiment was performed at the RI Beam Factory operated by RIKEN Nishina Center and CNS, University of Tokyo. The authors acknowledge the RIKEN accelerator staff for their support. This work was supported by JSPS KAKENHI Grant Nos. JP23244060, JP24740180, JP26247044, JP15H02096, JP17H01132, JP17H06090, and JP18H03711.

## References

- [1] Burbidge E.M. et al., *Rev. Mod. Phys.*, 1957;29:547.
- [2] Hirayama Y. et al., *Nucl. Instrum. Method B*, 2015;353:4.
- [3] Hirayama Y. et al., *Nucl. Instrum. Method B*, 2017;412:11.
- [4] Kudryavtsev Yu. et al., *Nucl. Instrum. Method B*, 1996;114:350.
- [5] Dasso C.H. et al., *Phys. Rev. Lett.*, 1994;73:1907.
- [6] Watanabe Y.X. et al., *Phys. Rev. Lett.*, 2015;115:172503.
- [7] Mukai M. et al., *Nucl. Instrum. Method A*, 2018;884:1.
- [8] Hirayama Y. et al., *Nucl. Instrum. Method A*, 2021;997:165152.
- [9] Schury P. et al., *Phys. Rev. C*, 2017;95:011305(R).
- [10] Hirayama Y. et al., *Phys. Rev. C*, 2018;98:014321.
- [11] Watanabe Y.X. et al., *Phys. Rev. C*, 2020;101:041305(R).
- [12] Ahmed M. et al., *Phys. Rev. C*, 2021;103:054312.
- [13] Walker P.M. et al., *Phys. Rev. Lett.*, 2020;125:192505.
- [14] Watanabe H. et al., submitted to *Phys. Lett. B*.
- [15] Hirayama Y. et al., *Phys. Rev. C*, 2017;96:014307.
- [16] Mukai M. et al., *Phys. Rev. C*, 2020;102:054307.
- [17] Choi, H. et al., *Phys. Rev. C*, 2020;102:034309.
- [18] Huyse H. et al., *Nucl. Instrum. Method B*, 2002;187:535.
- [19] Kudryavtsev Yu. et al., *Nucl. Instrum. Method B*, 2013;297:7.
- [20] Bohr A, Mottelson B.R., *Nuclear structure:volume II Nuclear deformations*. Massachusetts(US):W.A. Benjamin, Inc.;1975.